Electronic Supplementary Information

for

A Ru-anthraquinone dyad with triple functions of PACT, photoredox catalysis and PDT upon red light irradiation

Chao Zhang,[ab] *Xusheng Guo,*[ab] *Xuwen Da,*[ab] *Zhanhua Wang,*[ab] *Xuesong Wang,*[*ab] *and Qianxiong Zhou*[*a]

[a] *Key Laboratory of Photochemical Conversion and Optoelectronic Materials, Technical Institute of Physics and Chemistry, Chinese Academy of Sciences, Beijing 100190, P. R. China. Fax: +86-10-62564049; Tel: +86-10-82543592;*

[b] *University of Chinese Academy of Sciences, Beijing 100049, P. R. China.*

E-mail: xswang@mail.ipc.ac.cn (X.Wang); zhouqianxiong@mail.ipc.ac.cn (Q. Zhou).

Experimental section

Methods

HPLC analysis

Ru1, **Ru2** and the biq (2,2'-biquinoline) ligands were analyzed with a Vanquish UHPLC series instrument using a Thermo Accucore Vanquish C18+ column (100 mm × 2.1 mm, 1.5 μm). Mobile phases: acetonitrile/water: 80/20 (v/v, containing 0.1% formic acid); flow rate: 0.1 mL/min; detection at 280 nm.

3 mmol **Ru1** were dissolved in 1 mL DMSO and then were diluted to 500 μM with water. The solution of each complex was separated into 2 vials. One vial was used to test the purity of the complex, and the other was used to investigate the photo-induced ligand dissociation. 2,2'-biquinoline was dissolved in DMSO and was diluted 10 fold by acetonitrile.

Preparation of the mother solution

Ru1 and **Ru2** were dissolved in DMSO to obtain the 1 mM mother solutions, which can be diluted in the required solvents with different concentrations.

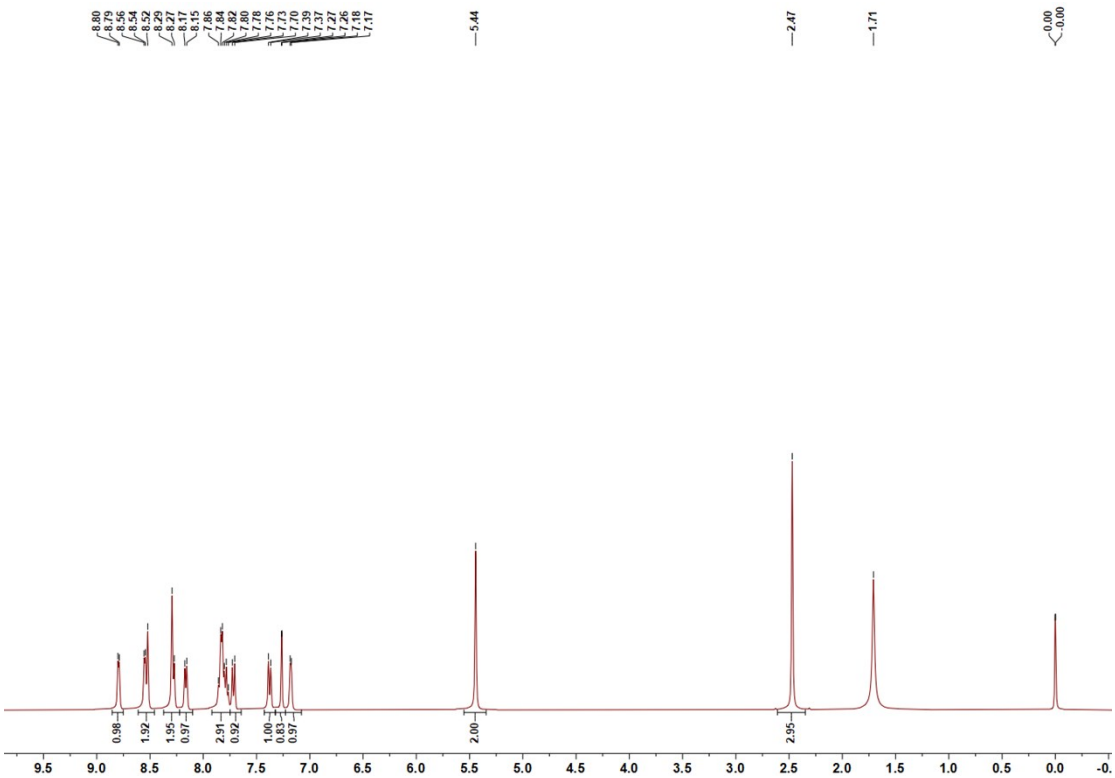

Fig. S1 ^{1}H NMR spectrum of NAbpy in $CDCl_3$.

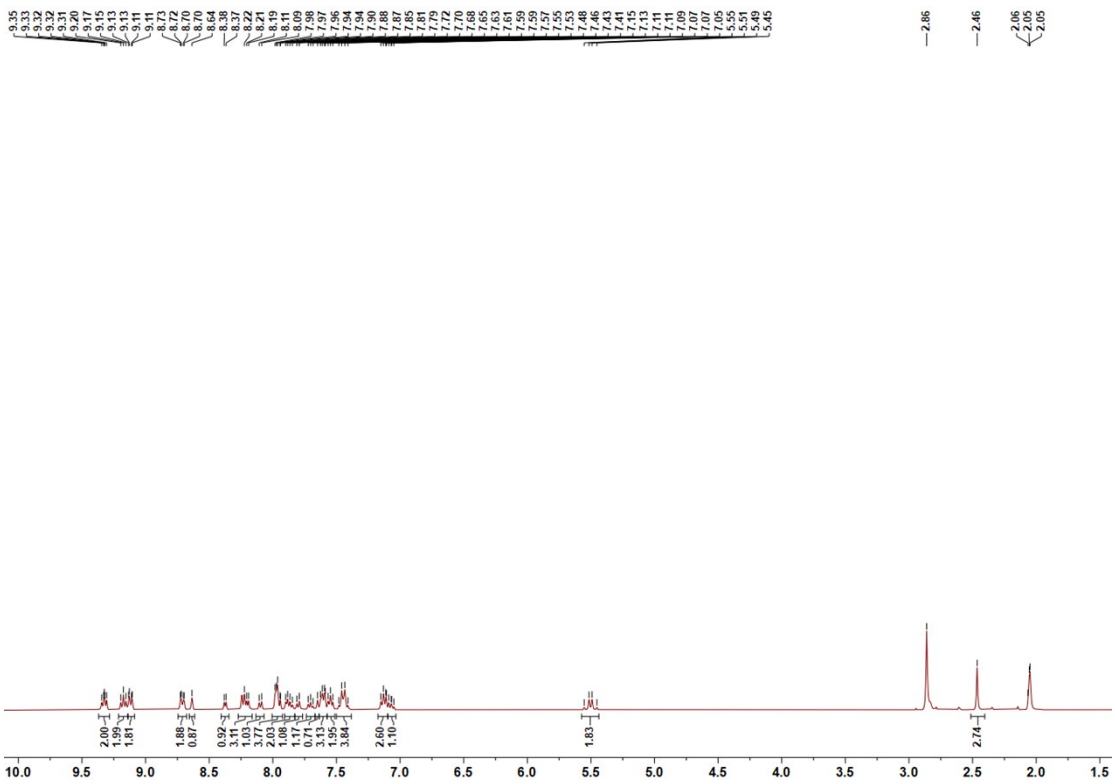

Fig. S2 ^{1}H NMR spectrum of **Ru1** in CD_3COCD_3.

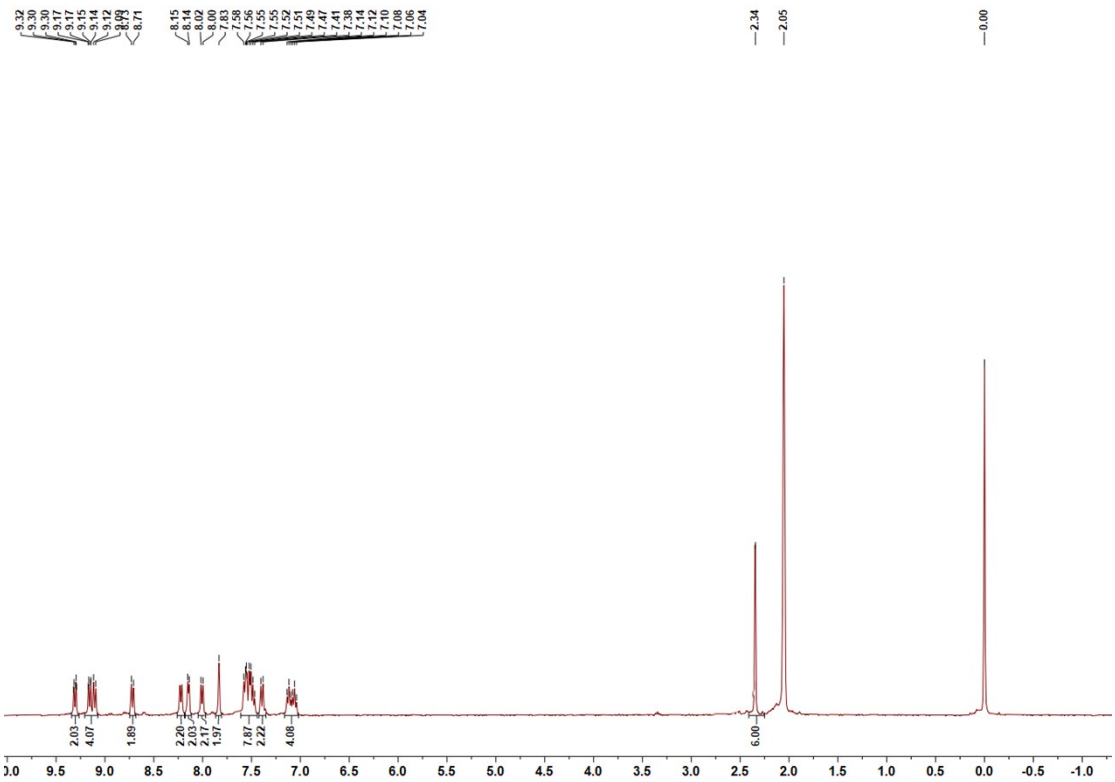

Fig. S3 ^{1}H NMR spectrum of **Ru2** in CD_3COCD_3.

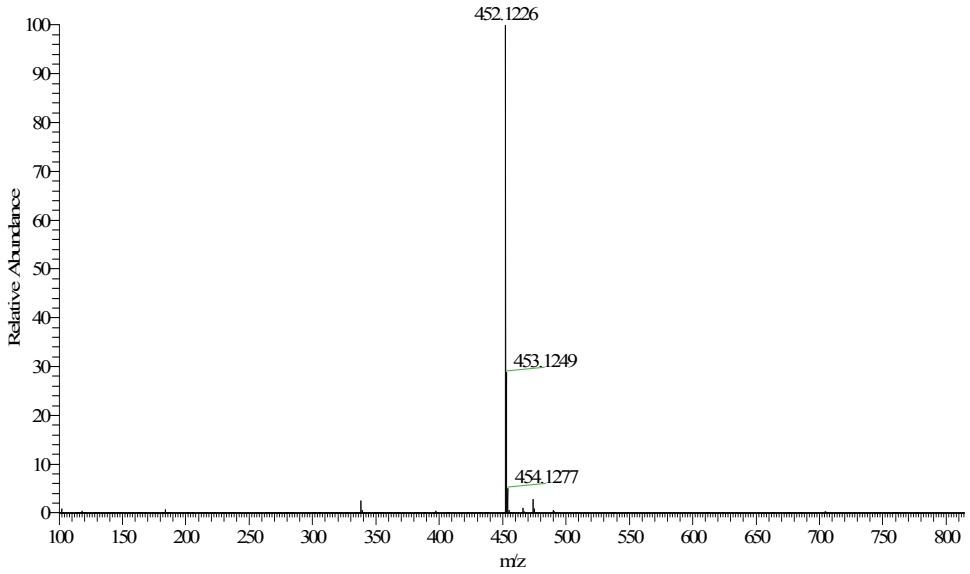

Fig. S4 ESI mass spectrum of **NAbpy**.

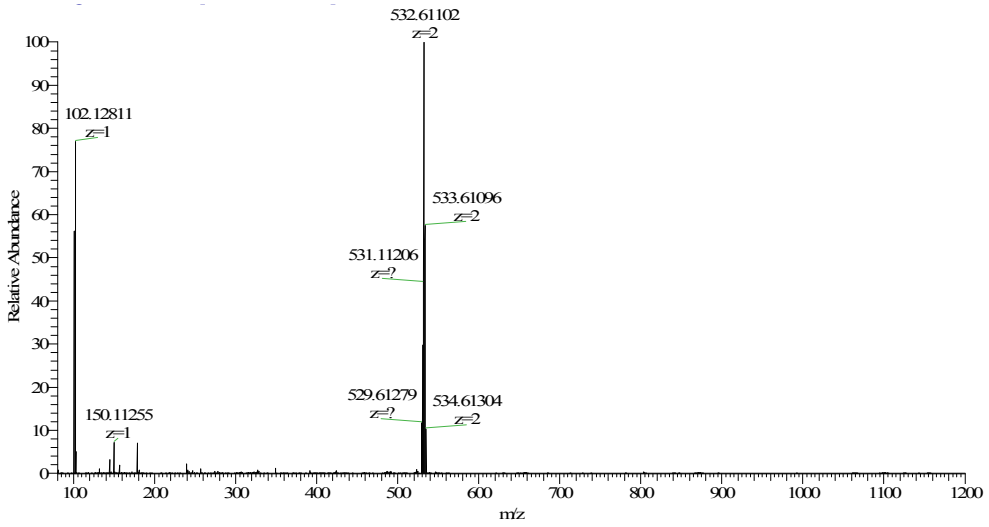

Fig. S5 ESI mass spectrum of **Ru1**.

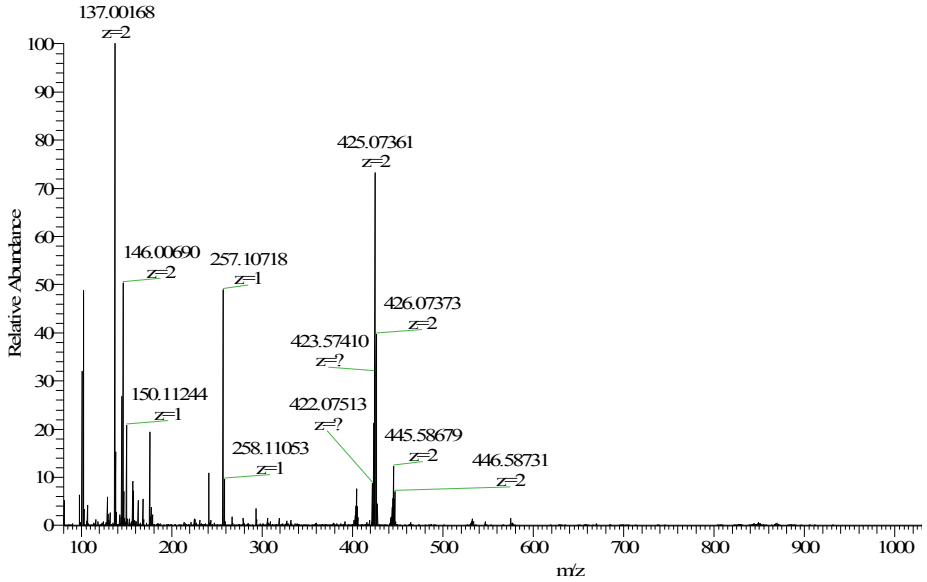

Fig. S6 ESI mass spectrum of **Ru1** after irradiation with a 600 nm LED (22.5 mW/cm^2) for 30 min. $[Ru(biq)(CH_3CN)_2(NAbpy)]^{2+}$ calculated: 445.58715, found: 445.58679; $[biq+H]^+$ calculated: 257.1007, found: 257.10718.

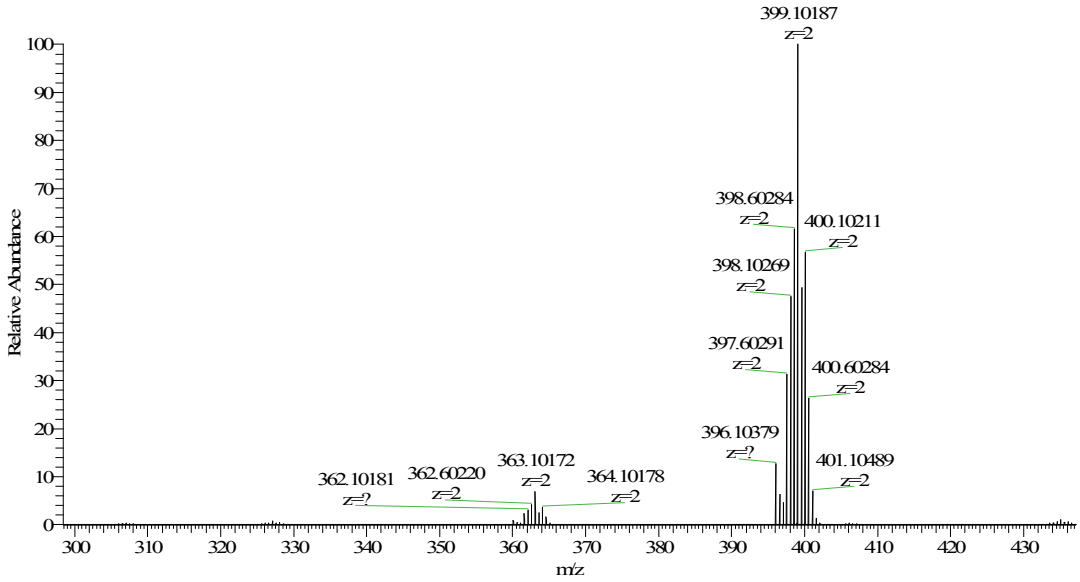

Fig. S7 ESI mass spectrum of **Ru2**.

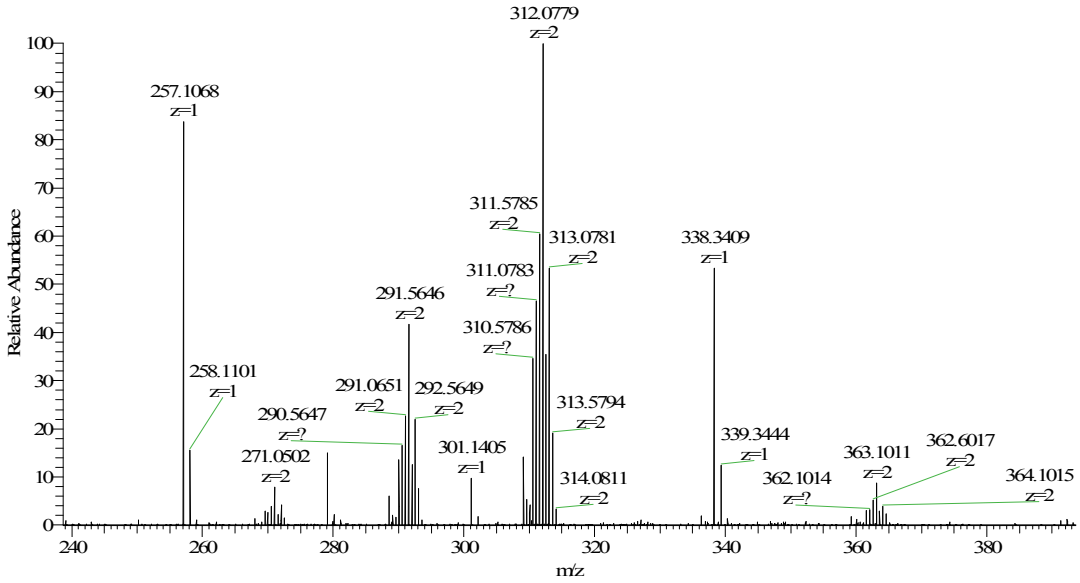

Fig. S8 ESI mass spectrum of **Ru2** after irradiation with a 600 nm LED (22.5 mW/cm^2) for 30 min. $[Ru(biq)(CH_3CN)_2(dmbpy)]^{2+}$ calculated: 312.0787, found: 312.0779; $[biq+H]^+$ calculated: 257.1007, found: 257.1068.

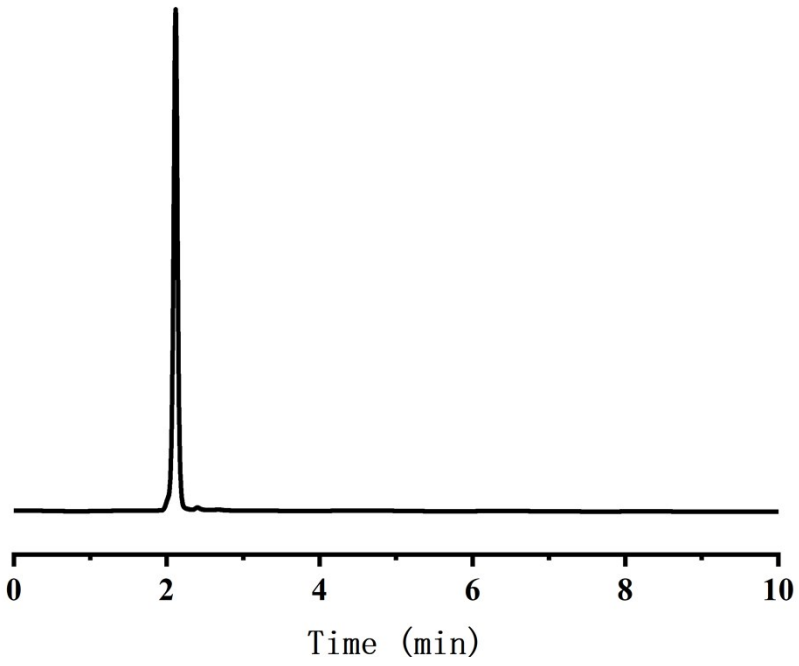

Fig. S9 HPLC chromatogram of **Ru1**.

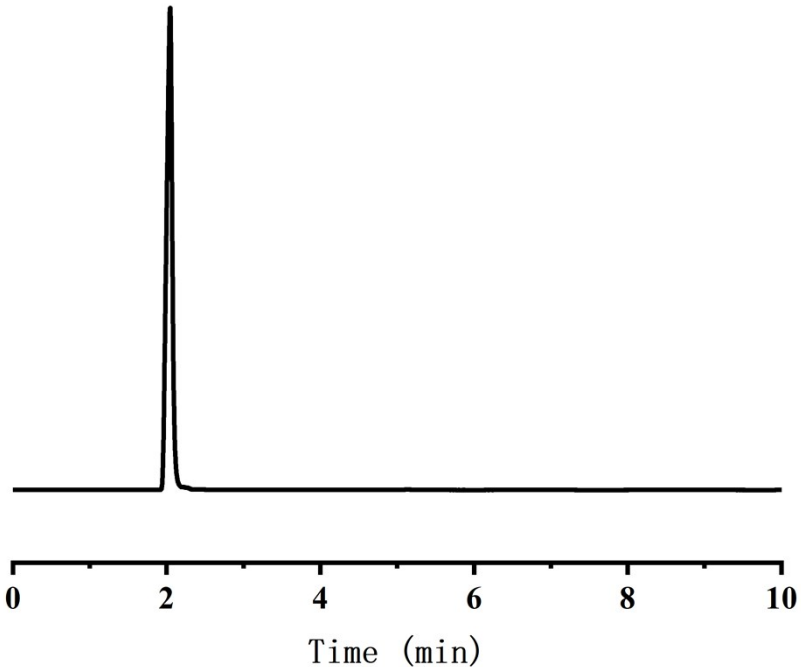

Fig. S10 HPLC chromatogram of **Ru2**.

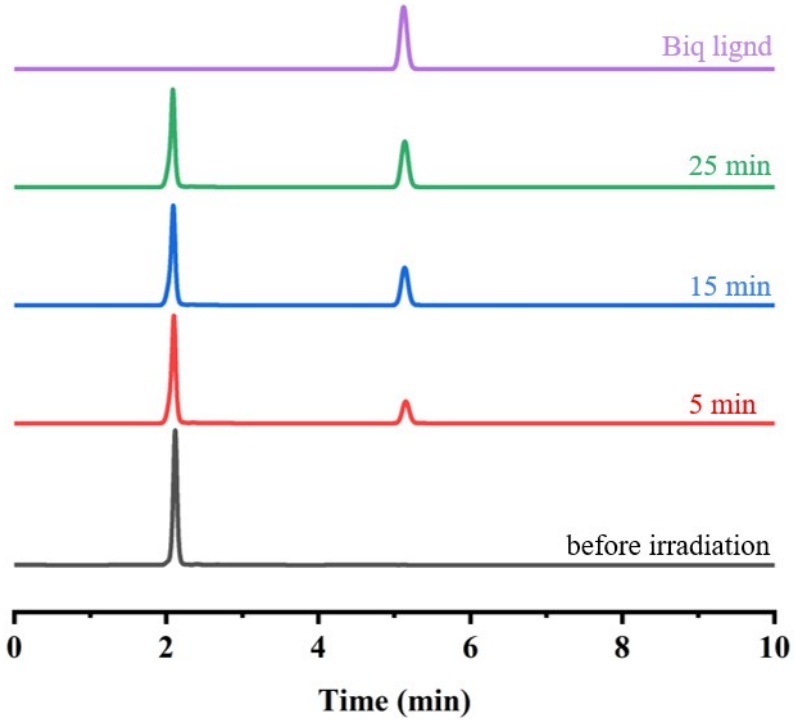

Fig. S11 Photo-induced (600 nm, 22.5 mW/cm^2) ligand dissociation of **Ru1** (500 μM in H_2O containing trace DMSO) investigated by HPLC.

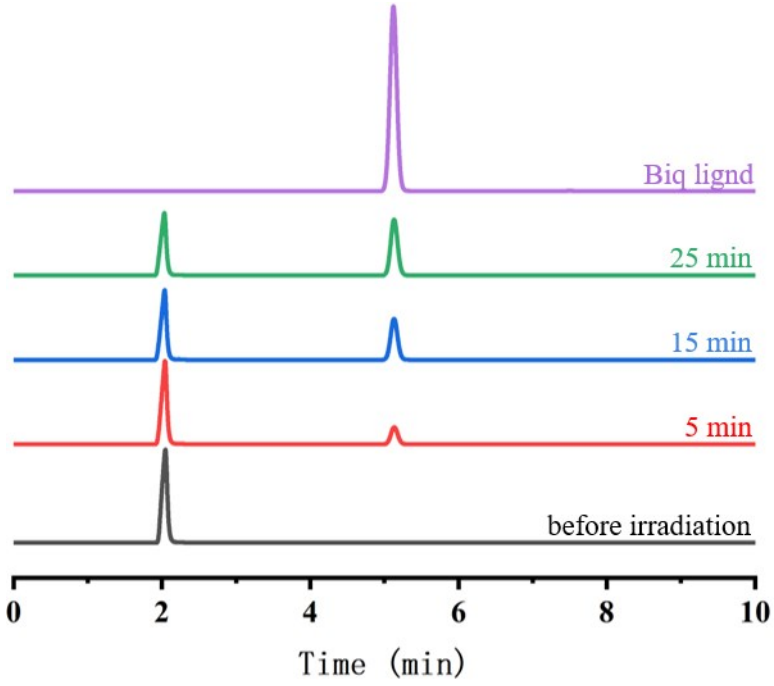

Fig. S12 Photo-induced (600 nm, 22.5 mW/cm^2) ligand dissociation of **Ru2** (500 μM in H_2O containing trace DMSO) investigated by HPLC.

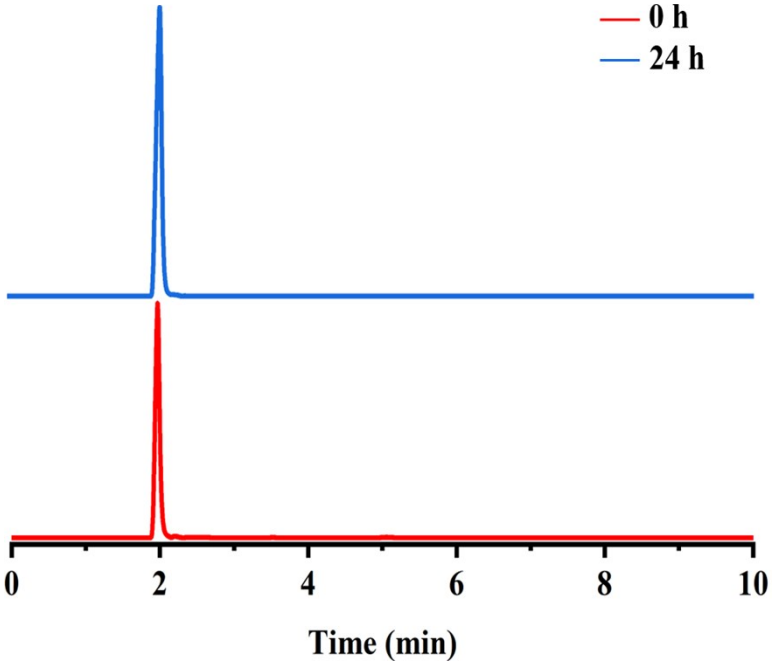

Fig. S13 Stability of **Ru1** (500 μM in PBS containing trace DMSO) in dark for 24 h investigated by HPLC.

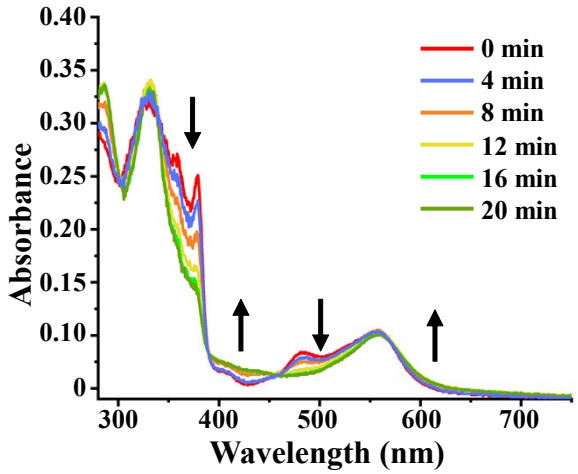

Fig. S14 Absorption spectra changes of **Ru2** upon 600 nm irradiation.

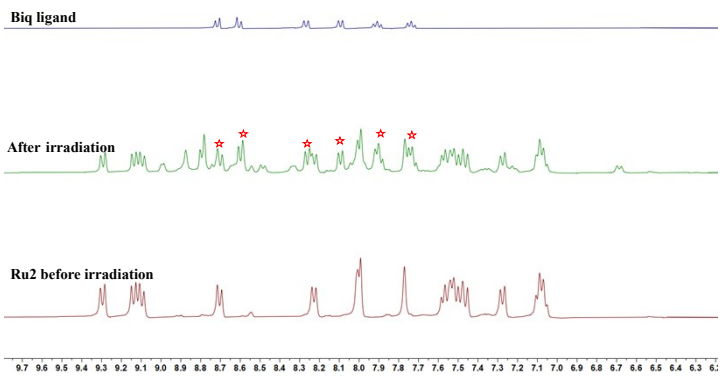

Fig. S15 ^{1}H NMR spectra of biq and **Ru2** before and after irradiation in CD_3COCD_3/D_2O = 2:1 (600 nm, 22.5 mW/cm^2). ☆ represents the signals of free biq ligand that has dissociated from the Ru center.

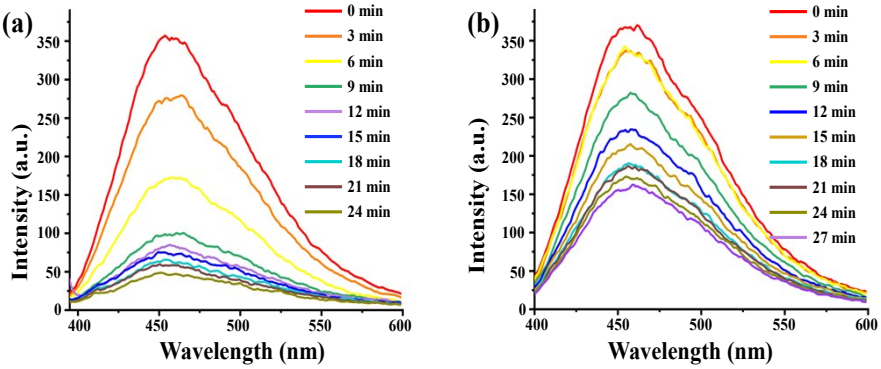

Fig. S16 (a) Emission (λ_{ex} = 360 nm) spectra changes of air-saturated H_2O solution of **Ru1** (10 μM) and NADH (200 μM) upon 600 nm LED irradiation (22.5 mW/cm^2). (b) Emission (λ_{ex} = 360 nm) spectra changes of air-saturated H_2O solution of **Ru1** aqua compound (10 μM) and NADH (200 μM) upon 600 nm LED irradiation (22.5 mW/cm^2).

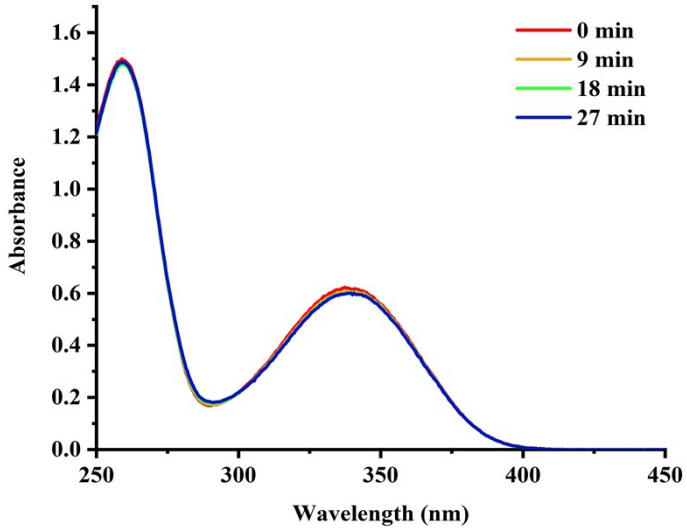

Fig. S17 Absorption spectra changes of NADH (200 μM in H_2O) upon 600 nm irradiation (22.5 mW/cm^2)

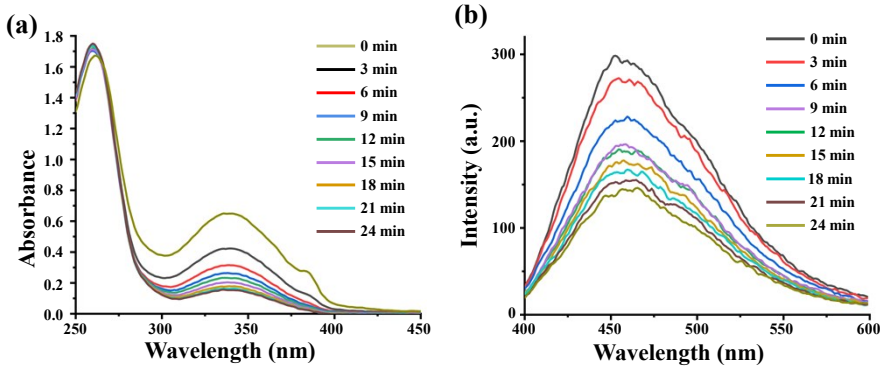

Fig. S18 Absorption spectra changes (a) and emission (λ_{ex} = 360 nm) spectra changes (b) of air-saturated H_2O solution of **Ru1** (10 μM) and NADPH (200 μM) upon 600 nm LED irradiation (22.5 mW/cm^2).

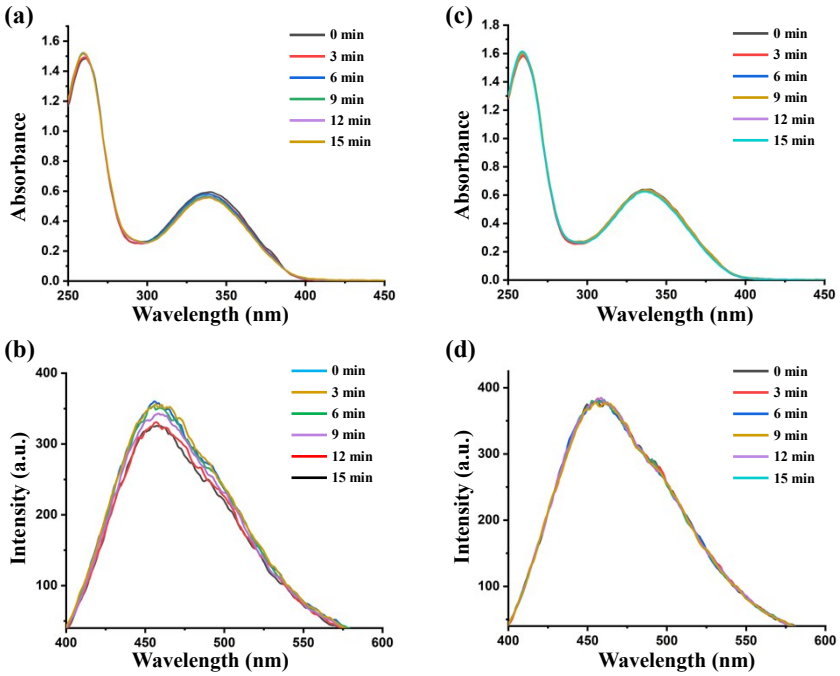

Fig. S19 Absorption (a) and emission (b) (λ_{ex} = 360 nm) spectra changes of air-saturated H_2O solution of **Ru2** (10 μM) and NADH (200 μM) upon 600 nm irradiation (22.5 mW/cm^2); Absorption (c) and emission (d) (λ_{ex} = 360 nm) spectra changes of air-saturated H_2O solution of **Ru2** aqua compound (10 μM) and NADH (200 μM) upon 600 nm LED irradiation (22.5 mW/cm^2).

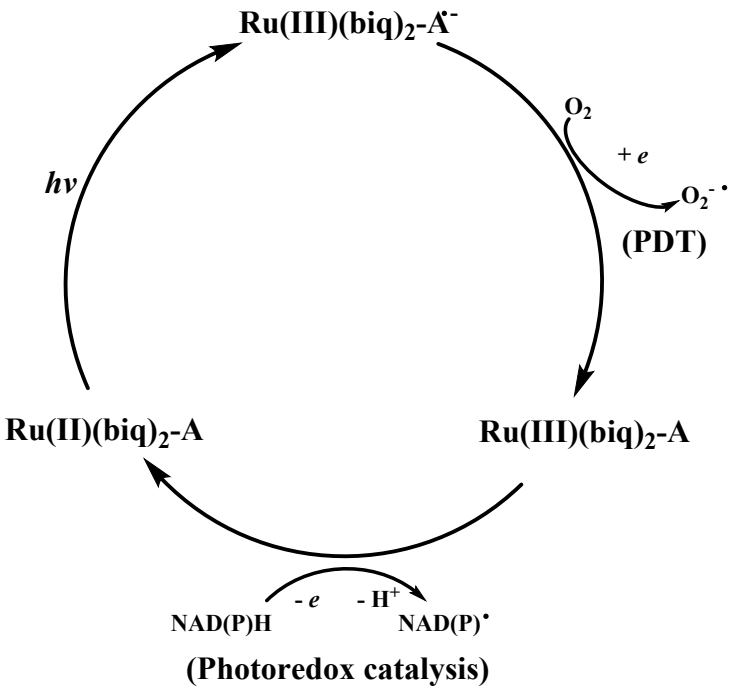

Fig. S20 Proposed photocatalytic cycle for NADH oxidation by **Ru1**.

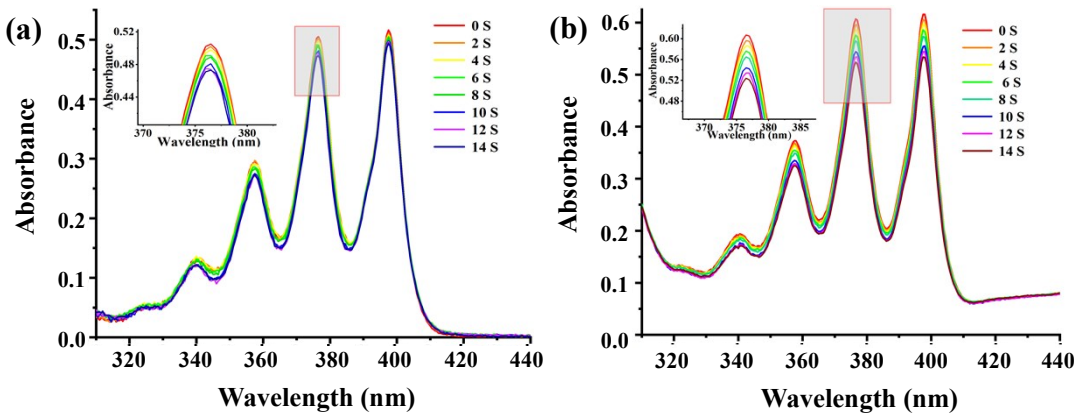

Fig. S21 UV-vis absorption spectra changes of 9,10-ABDA in the presence of (a) **Ru2**, (b) $[Ru(bpy)_3]^{2+}$ upon 470 nm irradiation (22.5 mW/cm^2). Inset is the enlargement of the spectra changes at 377 nm. The absorption change induced by the ligand dissociation of **Ru2** has been removed from the spectra by using it as the control.

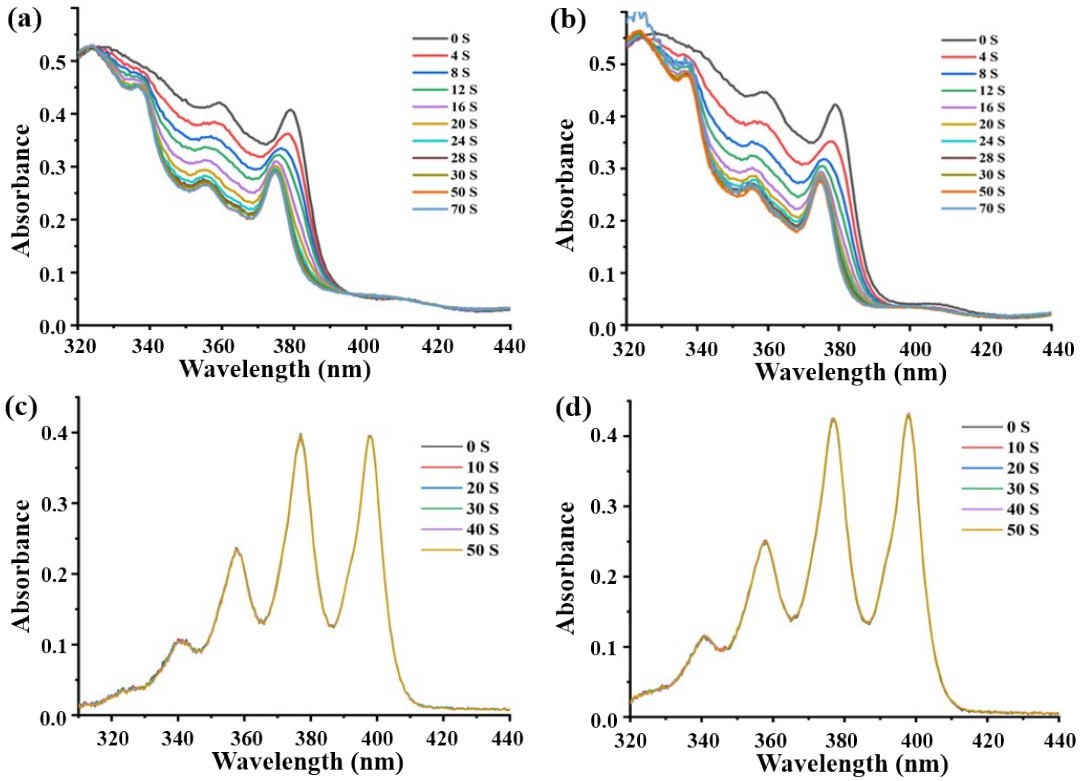

Fig. S22 UV-vis absorption spectra changes of **Ru1** (a) and **Ru2** (b) upon 470 nm irradiation (22.5 mW/cm^2) in CH_3CN. After irradiation for 100 seconds, 9,10-ABDA was added. (c) and (d) are the absorption bleaching of 9,10-ABDA by the photo-products of **Ru1** and **Ru2**, respectively, upon 470 nm irradiation (22.5 mW/cm^2).

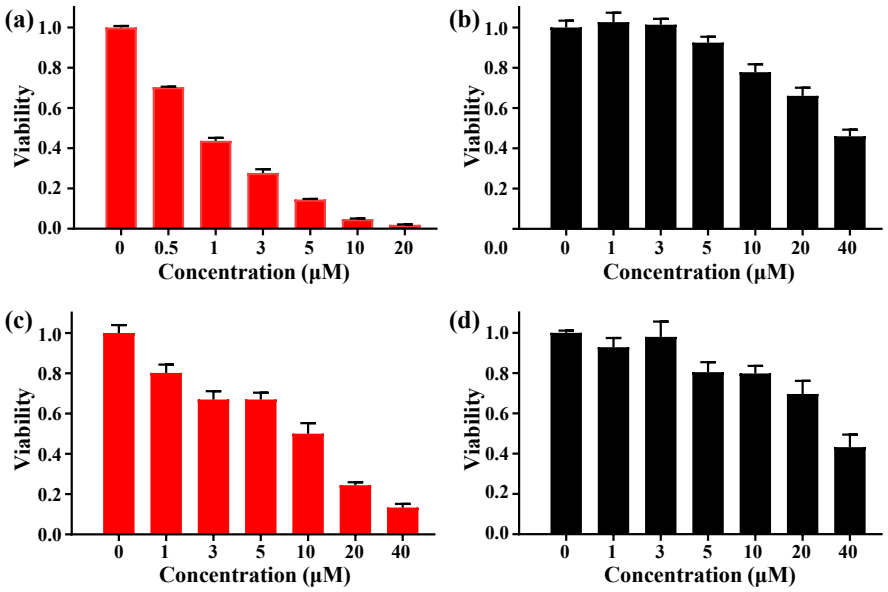

Fig. S23 Cytotoxicity of **Ru1** (a, b) and **Ru2** (c, d) towards A549 cells upon irradiation at 600 nm for 30 min (a and c, 22.5 mW/cm^2) or in the dark (b, d).

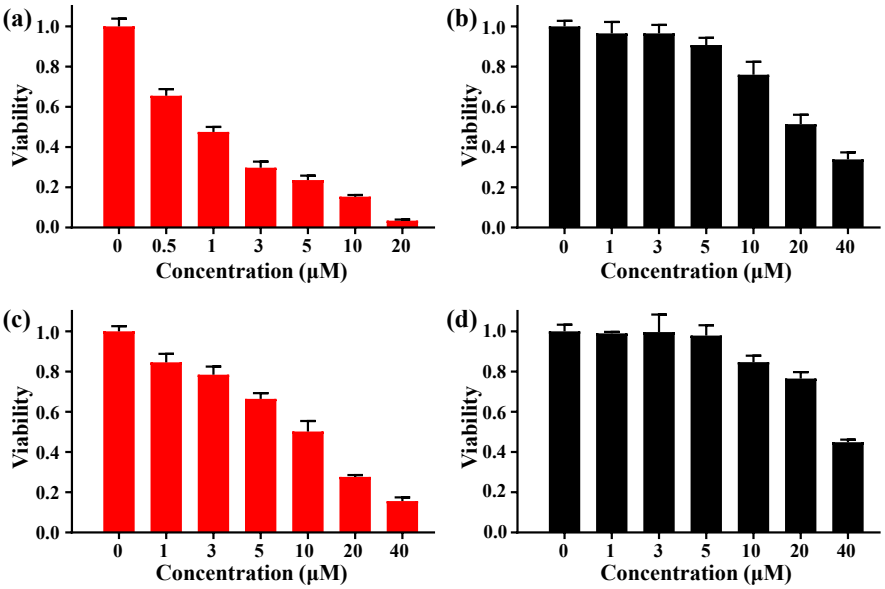

Fig. S24 Cytotoxicity of **Ru1** (a, b) and **Ru2** (c, d) towards A549/DDP cells upon irradiation at 600 nm for 30 min (a and c, 22.5 mW/cm^2) or in the dark (b, d).

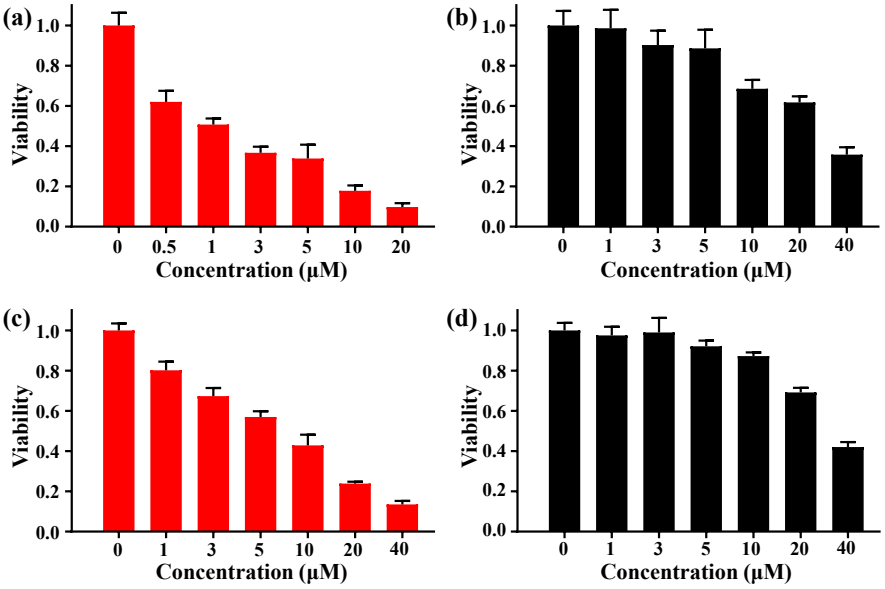

Fig. S25 Cytotoxicity of **Ru1** (a, b) and **Ru2** (c, d) towards SKOV-3 cells upon irradiation at 600 nm for 30 min (a and c, 22.5 mW/cm^2) or in the dark (b, d).

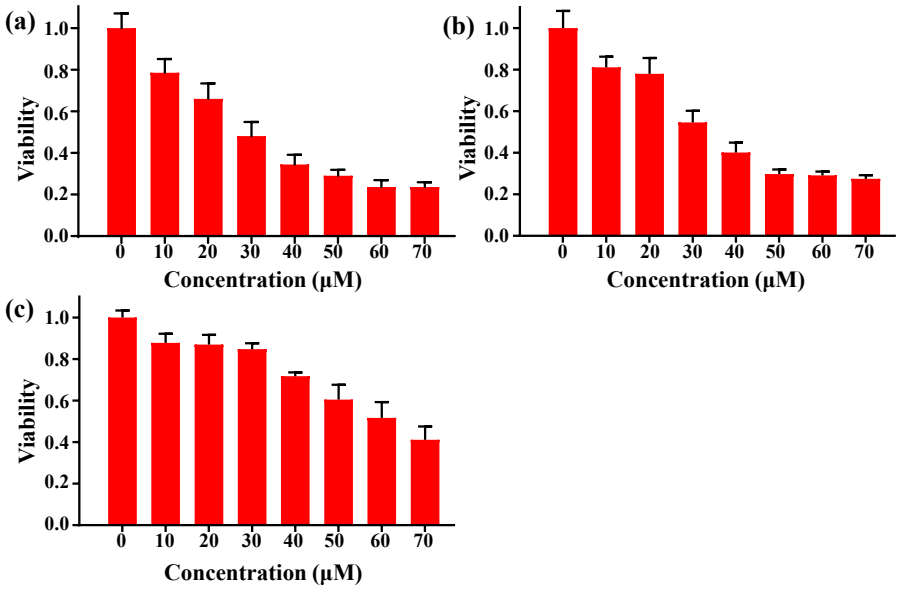

Fig. S26 Cytotoxicity of Cisplatin towards A549 (a), SKOV-3 (b) and A549/DDP (c) cells respectively in the dark.

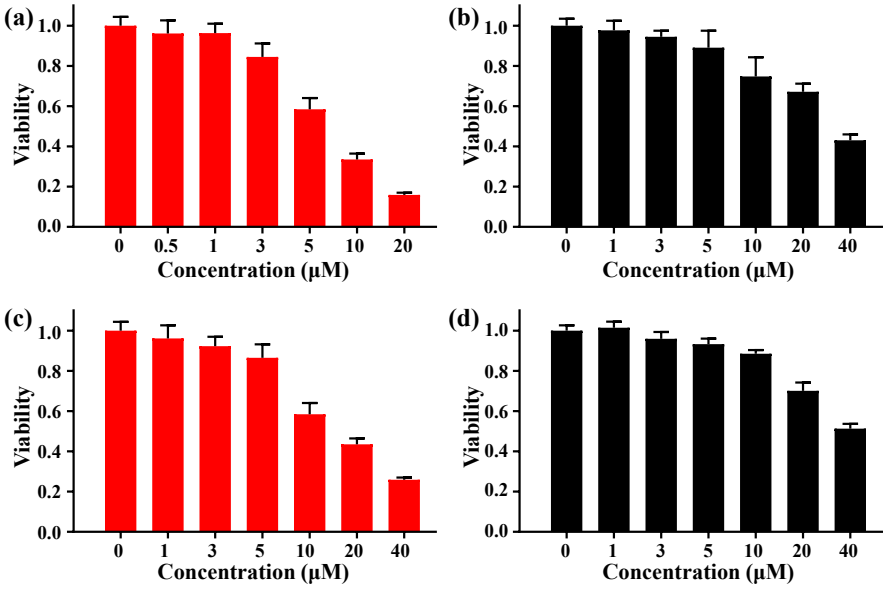

Fig. S27 Cytotoxicity of **Ru1** (a, b) and **Ru2** (c, d) towards A549 cells in hypoxia (3% O_2) upon irradiation at 600 nm for 30 min (a and c, 22.5 mW/cm^2) or in the dark (b, d).

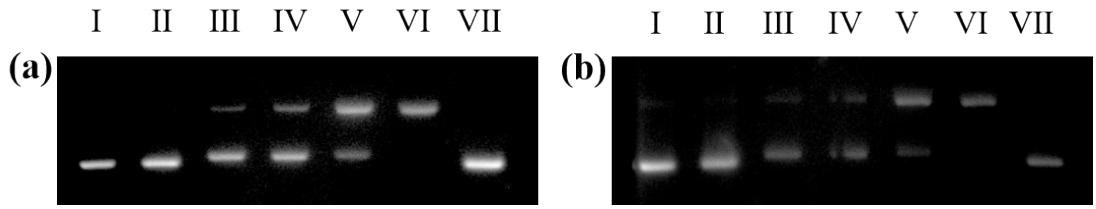

Fig. S28 Agarose gel electrophoresis pattern of pBR322 DNA (100 mM in base pairs) in tris-EDTA (5 mM, pH = 7.5) upon irradiation (600 nm) for 25 min in the presence of complexes **Ru1** and **Ru2** with varied concentrations. (a) Lane Ⅰ, DNA alone; lane Ⅱ, DNA+light; lane Ⅲ-Ⅵ, DNA+light+**Ru1** with concentrations of 1, 2, 3, 4 μM, respectively; lane Ⅶ, DNA+Ru1(4 μM) in the dark. (b) Lane Ⅰ, DNA alone; lane Ⅱ, DNA+light; lane Ⅲ-Ⅵ, DNA+light+**Ru2** with concentrations of 200, 400, 600, 800 μM; lane Ⅶ, DNA+**Ru2** (800 μM) in the dark.

Table S1. SKOV-3 cellular uptake, subcellular distribution and oil/water partition coefficients of **Ru1** and **Ru2**.

pmol/10^6cell [a)]	Nucleus	Cytoplasm	Mitochondria	Total	Log $P_{Ao/Aw}$
Ru1	20 ± 2	186 ± 22	165 ± 9	206 ± 22	1.25
Ru2	17 ± 0.7	160 ± 18	70 ± 3	177 ± 18	0.89

[a)] Measured by Ru content using inductively coupled plasma mass spectrometry (ICP-MS)

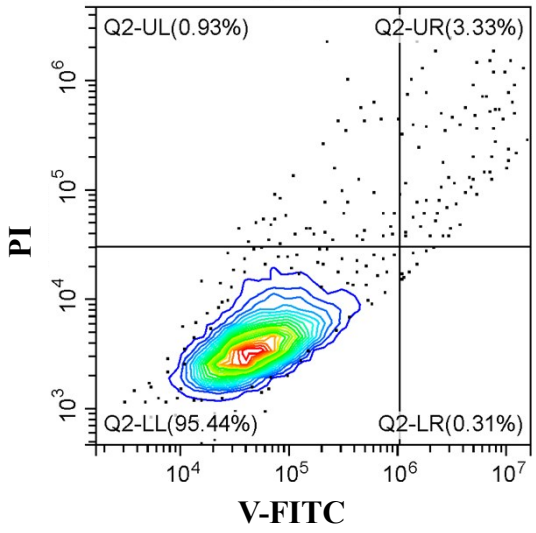

Fig. S29 Flow-cytometric analysis of SKOV-3 cells based on Annexin V-FITC and PI staining. The cells were only treated with irradiation for 30 min (600 nm, 22.5 mW/cm^2).

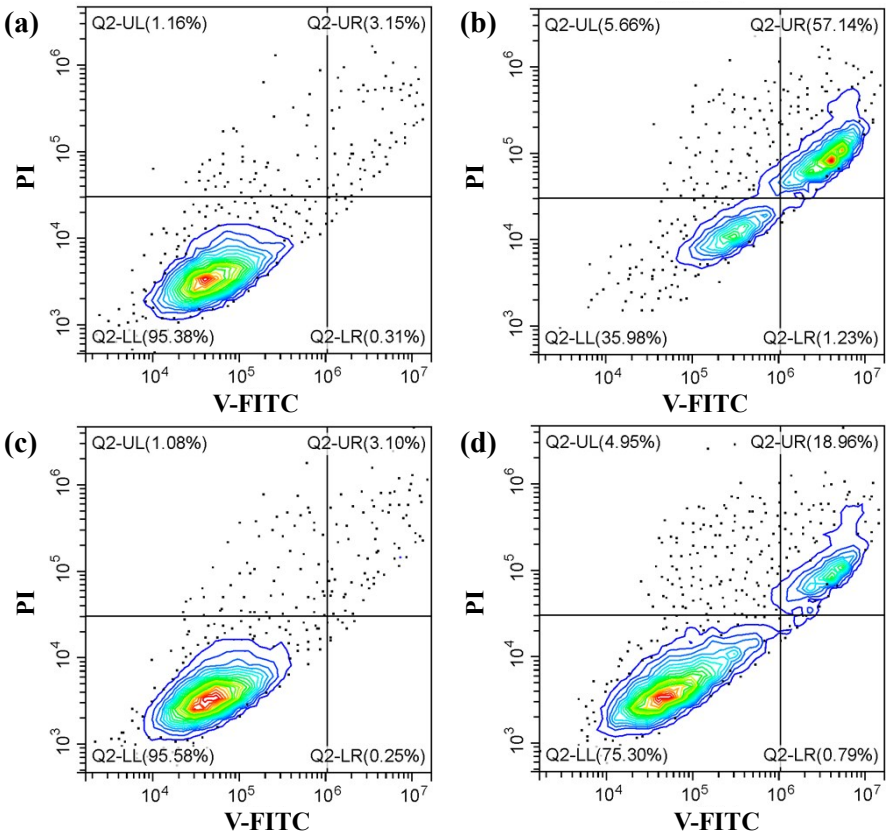

Fig. S30 Flow-cytometric analysis of SKOV-3 cells based on Annexin V-FITC and PI staining. The cells were treated with **Ru1** (1.5 μM, a and b) or **Ru2** (1.5 μM, c and d) in the dark (a, c), or with irradiation for 30 min (b, d) (600 nm, 22.5 mW/cm^2).

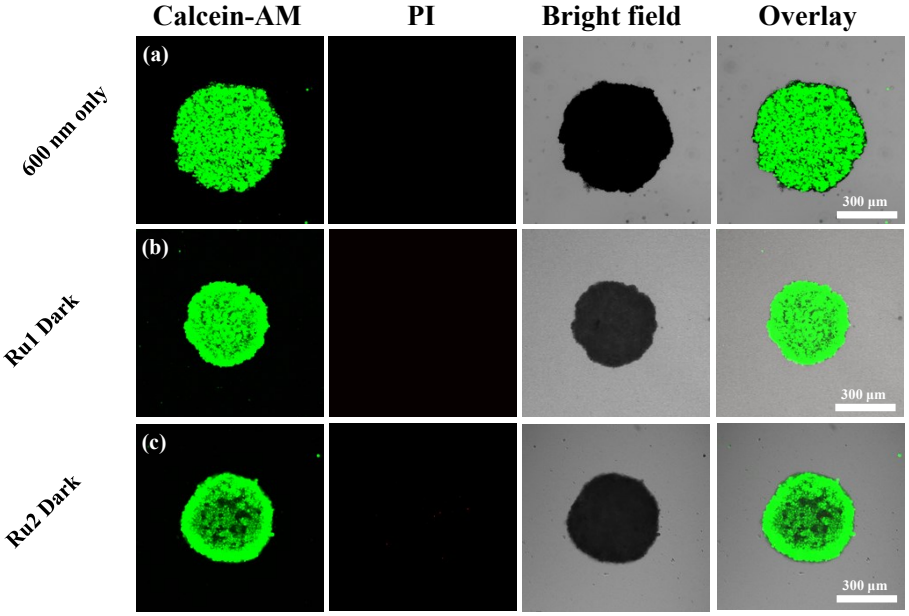

Fig. S31 (a) Images of SKOV-3 MCSs treated with irradiation (600 nm, 22.5 mW/cm^2) for 30 min; Images of SKOV-3 3D MCSs treated by **Ru1** (b) or **Ru2** (c) in the dark for 30 min and stained by Calcein-AM and PI. Scale bars: 300 μm.